Adsorption 3, 67–79 (1996)

Preparation and Characterization of Bimodal Porous Carbons Derived from a Styrene-Divinylbenzene Copolymer

WEIJIONG LI, THEODORE R. SEMONES, JIANPING LI AND ROBERT G. JENKINS
Department of Chemical Engineering, University of Cincinnati, Cincinnati, OH 45221, U.S.A.

Abstract. A styrene/divinylbenzene copolymer has been used as precursor for making porous carbons with bimodal pore size distributions (i.e., with both microporosity and mesoporosity). Pretreatment of the as-received copolymer by mild oxidation in air, significantly increased the carbon yield after carbonization. Reactivity studies of the polymer-based chars to CO_2 clearly show the influences of some important factors such as carbonization temperature, heating rate, soak time on char reactivities. Bimodal porous carbons were prepared by carbonization of the preoxidized styrene/divinylbenzene copolymer in N_2, followed by activation in CO_2 at different temperatures to different levels of burnoff. The pore structures of the porous carbons produced have been characterized by various techniques such as gas adsorption and mercury porosimetry. The surfaces of the porous carbons produced, and a commercial carbon adsorbent, have been modified with HNO_3 and H_2O_2 treatment at various conditions. Characterization of the surface oxygen functionality, both quantitatively and qualitatively, has been achieved using techniques such as Linear Temperature Programed Desorption (LTPD) and selective neutralization of bases.

Keywords: porous carbons, activation, oxidation, surface oxygen groups, LTPD

1. Introduction

There are very large quantities of waste plastic materials produced every year. Some of these plastics have the potential of making valuable porous carbons (Neely, 1981; Neely and Isacoff, 1982). Thus, these waste materials may be given a "second life" if they can be converted into value-added products such as adsorbents and catalyst supports. The main purpose of this study was to examine the potential of producing novel, highly porous carbons from a commercially available polystyrene resin.

It is known that linear polystyrenes, when thermally pyrolyzed, yield no carbonaceous material (Wall, 1970). Thus, they are not suitable for direct use as starting material to make porous carbons. However, crosslinked polystyrenes can be readily carbonized to carbonaceous residual, with carbon yield increasing with the crosslinking level (Winslow et al., 1955; Winslow and Matreyek, 1956). The most common method to crosslink the polymer chains is by sulfonation (Kawasumi et al., 1979), as is used to prepare "Ambersorb" adsorbents produced by Rohm and Hass Company (Neely, 1975). One problem of using sulfonation is that relatively large amounts of sulfur oxides are evolved during the pyrolysis of the polymer. The process to clean up these environmentally unacceptable compounds adds to processing costs. In this study, pretreatment of a linear styrene-divinylbenzene copolymer, to yield a highly crosslinked thermosetting polymeric material was carried out by mild oxidation with air. Using this method, the gaseous products evolved during pyrolysis will be mainly oxides of carbon and water, which are much more environmentally benign.

Most commercially available porous activated carbons are essentially microporous (5–10 Å). These carbons are often limited in a diffusional and

accessibility sense, especially when adsorption of relatively large organic molecules is involved, e.g., such as waste water treatment and hydrodesulfurization of heavy oils. In such situations, it is felt that porous carbons with bimodal pore size distribution would function better. That is, a large concentration of micropores offers most adsorption sites, and a substantial degree of meso- and/or macroporosity enhances transport of adsorptive molecules inside the particles. In this study, the concept of making bimodal porous carbons from a crosslinked styrene/divinylbenzene copolymer is based on the fact that the polymer already contains some quantity of mesopores. After pyrolysis, the mesopores will be maintained to a great extent if the polymer is truly thermosetting, and substantial amounts of micropores can be generated by thermal degradation and subsequent activation in, say CO_2, H_2O or air.

Besides the pore structure, the surface nature of porous carbons are also very important to their adsorptive and reactive properties. It is well known that the properties of the surface are determined by the presence of surface functional groups on the carbon's surface, of which oxygen-containing groups are the most abundant and, thus, critical to the carbon surface properties (Bansal et al., 1988). Surface oxygen groups are usually formed during chemisorption or reaction with oxygen-containing gases such as O_2, CO_2 or oxidants such as nitric acid and hydrogen peroxide (Hall et al., 1989). These oxygen groups occupy various sites on the carbon surface and exist in chemically and energetically different structures, depending on their formation mechanisms and the carbon surface.

The objectives of this investigation are: 1) to make novel porous carbons with bimodal pore size distribution from a styrene-divinylbenzene copolymer; 2) to study the effect of preparation conditions on the pore structure development of the resulting porous carbons; 3) to characterize these carbons using techniques such as char reactivities, thermogravimetric analysis (TGA), gas adsorption, mercury porosimetry, Scanning Electron Microscopy (SEM) and density measurements; 4) to characterize the carbon surface by studying its capacity of forming oxygen-containing surface groups at low temperatures and to follow changes of the groups, particularly the acidic ones, formed on the surface under various experimental conditions, using well-known indirect techniques such as Linear Temperature Programed Desorption (LTPD) and selective neutralization.

2. Experimental

2.1. *Starting Material*

Several ion-exchange resins and polymers were screened as potential precursors for novel carbon. Although yields of carbon were generally reasonable (25–50 wt%), many chars exhibit poor propensity for activation to high surface area materials. The most promising carbon precursor material was a styrene-divinylbenzene copolymer obtained from Polysciences, Inc. Thus, all carbons discussed in this paper were made from a mesoporous styrene-divinylbenzene copolymer (PS-DVB, 50% DVB). The particle size of the original polymer beads is approximately 640 μm (weight averaged diameter). Before carbonization in N_2, this carbon precursor was first oxidized in air at various conditions to produce highly crosslinked PS-DVB. Oxidation conditions were selected such that oxygen was chemisorbed onto the polymer surface in reasonable amounts but not under conditions which resulted in significant combustion, gasification or pyrolysis. The oxidation was conducted in a horizontal temperature programmable tube furnace (Lindberg Model 55341) with samples placed in an alumina boat. The sample layer in the boat was thin enough so that the reactions could take place homogeneously throughout the sample bed. These air-oxidized PS-DVB samples were then used as starting materials for making porous carbons. For purposes of comparison, a commercial porous carbon adsorbent Ambersorb 575 was also used in some parts of this investigation. It is well established that Ambersorb 575 has a distinct bimodal pore structure.

2.2. *Reactivity Study*

The reactivities of the polymer-based chars (carbonized PS-DVB) in CO_2 activation were studied to investigate the reactive nature of the carbon's surface and for tailoring appropriate preparation conditions for activating porous carbons, i.e., selectively gasify the carbon to yield high surface area. The study was conducted by using a thermogravimetric analyzer (Model 951, Du Pont Instruments). Sample size was very small (~30 mg) and the gas flow rate through the sample chamber was high enough (200 cm^3/min) so that mass transfer resistance between gas film and particle surface were eliminated during the C-CO_2 reaction. The effects

of some important preparation parameters including carbonization temperature, soak time, heating rate of carbonization, and activation temperature, on the char reactivity were studied. The chars were obtained by carbonization of the preoxidized PS-DVB in N_2 at 900 to 1000°C with heating rate from 5 to 50°C/min. and soak time from 0.5 to 1.5 h. Reaction temperatures in CO_2 ranged from 750 to 850°C.

For reactivities of chars during gasification, several parameters have been used in literature. In this study, the reactivity is expressed as two parameters (Jenkins et al., 1973). The first one reactivity (R_T) is a measure of the maximum rate and is given by

$$R_T = -\frac{1}{w} \times \frac{dw}{dt}$$

where R_T is reactivity [g/(min · g)], w the starting weight of char (g), and dw/dt the maximum rate of reaction (g/min). The second measure is $\tau_{0.5}$ which is the time to reach 50% burnoff and is a useful parameter to describe the overall reactivity of the char. As $\tau_{0.5}$ increases, the char's reactivity decreases.

2.3. *Preparation of Porous Carbons*

Production of the chars was performed in the same tube furnace used for PS-DVB preoxidation. The preoxidized PS-DVB samples were heated in N_2 from 100°C to 950°C at a heating rate of 10°C/min, and soaked at 950°C for 30 minutes. The carbonized samples were then subjected to the subsequent activation in CO_2 at both 800 and 850°C (samples designated PS-DVB-800 and PS-DVB-850, respectively) for various times to obtain different levels of carbon removed (burnoff) from zero to 87 wt%. The carbonized sample was kept in an atmosphere of nitrogen before flowing gas through the tube was switched to activating agent (CO_2) when activation temperature was reached. Gas flow rate during carbonization and activation was 950 cm^3/min, sufficient to minimize film diffusional limitations.

2.4. *Characterization of Porous Carbons*

2.4.1. Pore Structure. Porous carbons were first characterized for their pore structures and surface areas. Nitrogen adsorption at 77 K at relative pressure (p/p_0) ranging from 10^{-4} to 0.35 was performed using a surface area analyzer (Gemini 2360, Micromeritics). Isotherms were interpreted using the Dubinin-Radushkevich equation (Dubinin, 1966, 1975) to calculate the micropore structural parameters. Also, BET surface areas were obtained. Some selected samples were used to measure the micropore distributions using Horvath-Kawazoe equation (1983) from N_2 adsorption data (p/p_0 from 10^{-7} to 0.1) obtained using an Accelerated Surface Area and Porosimetry System (ASAP2000, Micromeritics).

Mercury porosimetry was used to characterize the meso- and macroporosity. A mercury porosimeter (Autoscan-60, from Quantachrome Corp.), with highest intrusion pressure of 60,000 psi, measuring pores with diameters from 36 Å to 44,000 Å was employed. It was found from gas adsorption data, for some selected samples, that porous carbons made in this study contain very few pores with diameters between 20 Å and 36 Å, therefore, for convenience, pores smaller than 36 Å are reported as micropores, even though, strictly, they include both micropores and mesopores following IUPAC classification (Gregg and Sing, 1982). Pores between 36 Å and 500 Å are reported as mesopores, and pores larger than 500 Å, macropores. Other techniques such as Scanning Electron Microscopy (SEM) and density measurements (water densities) were also performed for characterization. SEM studies were done using a Stereoscan 600 apparatus from Cambridge. Water densities were obtained at 20°C using Fisherbrand Gay-Lussac specific gravity bottles (10 ml).

2.4.2. Surface Characterization and Modification. Selected porous carbons were subjected to various oxidation and heat treatments in order to introduce oxygen complexes onto the carbon surface. The carbon surface was then characterized for its surface oxygen groups and acidity using Linear Temperature Programed Depsorption (LTPD) and selective neutralization techniques. Porous carbons were first oxidized in concentrated nitric acid or 30% (by weight) hydrogen peroxide solution at different temperatures (20–60°C) for different times (1–24 h). After oxidation, the samples were washed by excessive deionized water and dried at 110°C overnight. The LTPD experiments were conducted in a horizontal tube furnace (same as used for preparing the porous carbons) connected to a gas chromatograph (Varian 3300, from Varian Chromatography Systems) with a TCD detector. The sample was placed in a boat and dried again in He (flowrate ~ 40 cm^3/min) at 110°C for 2–3 h before a run began. A linear temperature program was applied to increase the temperature from 110°C to 1000°C at a heating rate of

5°C/min. The gases evolved (CO_2, CO, H_2O, H_2) were monitored by gas chromatography.

In the selective neutralization experiments, a sample was immersed in separate solutions of NaOH, Na_2CO_3, and $NaHCO_3$ (0.1 N to 0.2 N) in a volumetric flask placed in a 60°C waterbath for 24 h. Prior work indicated that 24 h contact time was sufficient to reach equilibrium. The remaining concentration of Na^+ not exchanged with H^+ was determined by titration with a 0.1 N standard HCL solution. The acidic oxygen groups present on the carbon surface can then be calculated by difference.

3. Results and Discussion

3.1. Preoxidation

Preliminary oxidation experiments in the TGA indicated that 250°C was an appropriate temperature for oxidative pretreatment. At that temperature the rate of oxidation was sufficiently slow that significant gasification, pyrolysis or combustion did not occur, yet it was rapid enough for measurements to be made in a reasonable time frame. Figure 1 is an oxidation curve for PS-DVB from an isothermal TGA run at 250°C in air. Similar behavior has been noted before in the low-temperature oxidation of coals (Cronauer et al., 1983). The TGA curve has three distinct regions. First there appears to be a period of about 25 min. during which the weight of the sample does not change. This indicates that there is either no interaction between the oxygen and the PS-DVB, or that the rate of uptake of oxygen is exactly matched by the rate of desorption of species derived from the interaction.

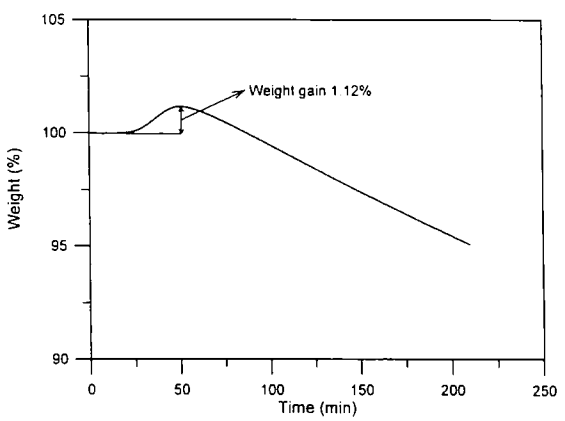

Figure 1. TGA curve of weight change during preoxidation of PS-DVB (in air at 250°C).

Since there was no attempt to analyze the effluent gas stream, it is impossible to determine which mechanism is occurring during this first phase of the process. Following this apparent induction period, there is a well defined region in which there is an appreciable net weight increase. The weight increases steadily until the apparent weight gain reaches 1.12 wt%, after which it declines monotonically (Fig. 1). After about 90 min. from the start of the experiment the weight of the sample is less than the original weight and further treatment continues the apparent weight loss.

These results suggest a mechanism in which the initial uptake of oxygen is a result of formation of functional groups such as peroxides, phenols and/or direct addition of oxygen atoms as bridges between the polymer units. However, since some of the added functional groups are relatively unstable (e.g., peroxides), they will decompose, presumably yielding water, and possibly oxides of carbon. The condensation of -OH type groups will, of course, lead to further crosslinking of the polymer units. Thus, following the induction period, one is observing the net weight changes which result as a consequence of oxygen being added to the sample and mass loss due to decomposition of oxygen-containing groups. Obviously, the data shown in Fig. 1, show that between 25 and 50 min. the chemisorption of oxygen dominates, and following that the reactions that result in a mass loss dominate. It should be noted that since the chemisorption is exothermic then localized "hot-spots" may occur, possibly leading to some limited pyrolysis reactions.

Preoxidation at 250°C of the original PS-DVB prior to subsequent carbonization does enhance its thermosetting properties. Thus, as will be seen, the carbon yield is increased and the original mesoporous structure is maintained. Thermogravimetric data, up to 950°C, obtained in N_2 clearly indicates the substantial influence of preoxidation on carbon yield. The as-received PS-DVB yields only 13.1 wt% char on pyrolysis to 950°C. However, char yields for preoxidized samples with oxidation times of 1.5, 2.0, and 4.0 hours at 250°C are 21.0, 34.2 and 41.1 wt% respectively, see Fig. 2. Mild oxidation in air for 4 hours at 250°C causes the char yield to more than double, in spite of a slight weight loss (~5 wt%) during the treatment. This observed substantial increase in carbon yield is a direct result of increased levels of crosslinking in the PS-DVB.

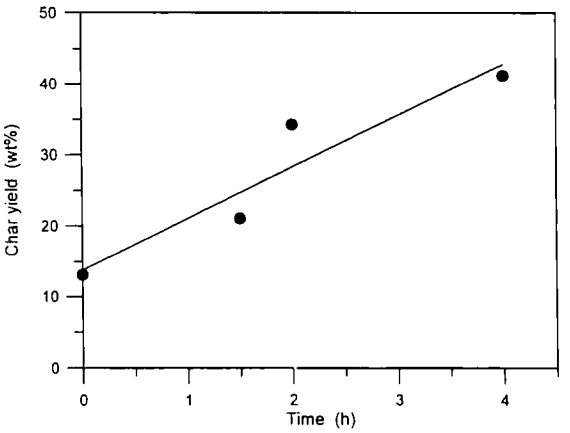

Figure 2. Influence of oxidation time on char yield from PS-DVB carbonized to 950°C.

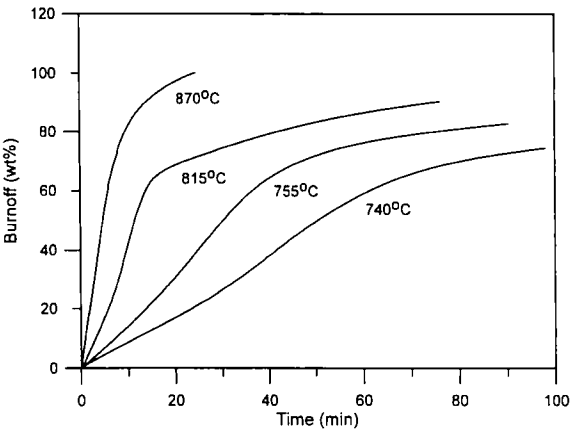

Figure 3. Influence of reaction temperature on reactivity of PS-DVB char in CO_2.

3.2. *Reactivity*

Carbon atoms located at the edges of the aromatic carbon layers generally control the reactivity of carbonaceous solids to O_2, CO_2, H_2O, and H_2, though other factors, such as diffusion limitations on the reactive gas to the reaction sites, and presence of catalytically active impurities may also play substantial roles in gasification processes (Walker et al., 1959). In addition, treatment conditions used during char preparation influence the subsequent char gasification reactivity.

Reactivity data in CO_2 were obtained for series of PS-DVB chars prepared at different conditions. In the first set of experiments, the 900°C heat-treated char (heating rate 10°C/min; soak time, 0.5 h) was reacted at temperatures ranging from 740°C to 870°C. Figure 3 shows the burnoff (BO) vs. time curves for the different reaction temperatures for this sample. The rates increase significantly with temperature, as expected. All the curves essentially have the same shape and three distinct regions can be found on each curve. These three regions indicate that the reaction rate first increases slowly with time, then passes through a maximum, and finally decreases slowly over a long period of time. This behavior concerning the reaction of microporous chars can be broadly explained by three different situations involved in the microporosity and surface area development during activation, i.e., i) opening of initially closed pores inaccessible to CO_2; ii) open pores and surface area then allow for easy access to the surface during further reaction; and, iii) finally the pore walls are consumed at high burnoff levels, leading to large pores, reduced area and reactivity (Mahajan and Walker, 1978). Therefore, it is very critical to choose appropriate activation temperature and time so that activation can reach the right stage to develop extensive porosity and surface area for the porous carbons being produced. The calculated reactivity data (R_T and $\tau_{0.5}$) also clearly show the increases in maximum and overall reactivity with increasing temperature (Table 1; Runs 1–4).

By assuming that the gasification reaction of char with carbon dioxide can be approximated as a first-order reaction, with respect to the weight of char, an apparent activation energy of 82 kJ/mol is calculated based on the data in Fig. 3 and by the application of the Arrhenius equation. This value is relatively small when compared with the activation energies reported for the chemical step of gasification, namely 200–300 kJ/mol (Laurendau, 1978; Salinas-Martínez de Lecea et al., 1990). This is probably due to interparticle diffusion limitations and deficiencies in assuming first-order behavior.

For other chars derived from PS-DVB, it can be seen that reactivity decreases with increase in carbonization temperature (Table 1; Runs 5–7). This trend is well established since higher carbonization temperature leads to increasing pyrolysis and reduced active site concentration. Table 1 also shows the effects of soak time at maximum heat treatment temperature, and heating rate on the char reactivity. A substantial decrease in reactivity with increasing soak time can be seen (Runs 5, 10 and 11). Increasing soak time at a given temperature results in small chemical changes to more carbonaceous material and "annealing" of active sites.

Table 1. Influence of reaction conditions on reactivity of PS-DVB char in CO_2.

Run no.	Carbonization temperature (°C)	Heating rate (°C/min)	Soak time (h)	Reaction temperature (°C)	R_T (g/min·g)	$\tau_{0.5}$ (min)
1	900	10	0.5	740	1.13	50.7
2	900	10	0.5	755	1.93	30.3
3	900	10	0.5	815	5.89	11.5
4	900	10	0.5	870	10.70	4.76
5	900	50	0.5	850	9.61	6.63
6	950	50	0.5	850	8.40	8.92
7	1000	50	0.5	850	1.35	32.6
8	900	5	0.5	850	12.1	8.65
9	900	20	0.5	850	10.9	6.35
10	900	50	1	850	6.65	8.68
11	900	50	1.5	850	2.31	31.5

The effect of heating rate on reactivity of the 900°C PS-DVB char is modest but somewhat complex. Examination of the relevant data (Table 1; Runs 5, 8 and 9) shows that reactivity, as measured by $\tau_{0.5}$, increases a little as the heating rate increases from 5°C/min to 20°C/min. Further increase in heating rate to 50°C/min has essentially no influence on reactivity. These observations reflect the fact that overall the structures of the chars prepared at higher heating rates are more disordered than those produced at 5°C/min. On the other hand, maximum reactivities (R_T) exhibit a small decrease as heating rate increases. These data, of course, only represent maximum values of reactivity and not representative of the overall behavior.

The reactivity studies show the reactive nature of the polymer-based chars and give useful information for selecting appropriate conditions for preparing porous carbons. In addition, these studies yield important information as to influences of variables such as ultimate carbonization temperature, heating rate and soak time at the final temperature.

3.3. *Pore Structure of Porous Carbons*

Figure 4 illustrates the change of nitrogen BET surface area of the porous carbons as a function of burnoff. Both curves for PS-DVB carbons, activated at 800 and 850°C, show maximum values, indicative of pore widening and collapse of the pore structure, at moderately high burnoff (50–70 wt%). Also in Fig. 4, it can be seen that the BET surface areas for PS-DVB-800 carbons are similar to PS-DVB-850 up to 50% burnoff, indicating that activation temperature, in the range studied, has small influence on the resulting carbons. However, at conversions greater than 60% BO there is a dramatic drop in surface area for the PS-DVB-800 carbons. A similar trend is observed at a somewhat higher burnoff (~70% BO) for the PS-DVB-850 chars.

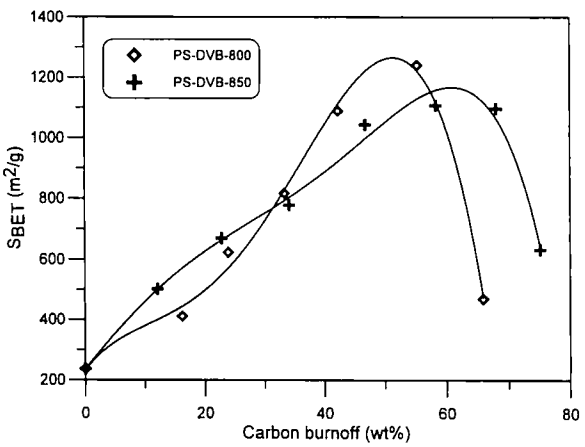

Figure 4. Variation of BET surface area with burnoff for PS-DVB carbons reacted with CO_2 at 800 and 850°C.

Physical adsorption of gases and vapors by activated carbons can be well described by the Dubinin-Radushkevich (D-R) equation (Dubinin, 1966, 1975):

$$W = W_0 \exp\left[-\left(\frac{A}{\beta E_0}\right)^2\right]$$

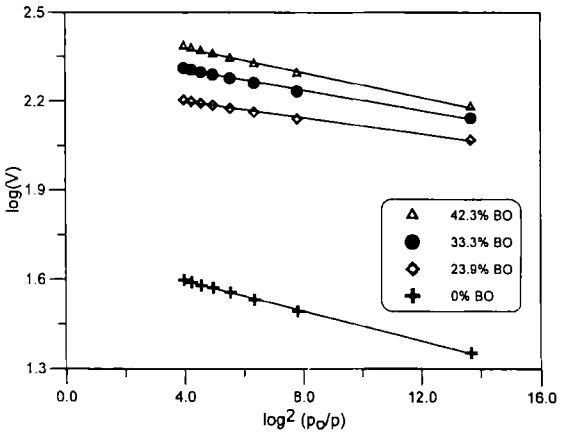

Figure 5. Dubinin-Radushkevich plots for PS-DVB-800 carbons.

where W_0 is the total volume of the micropores. From the familiar D-R plot, the parameters W_0 and E_0 can be obtained. Assuming slit-like pore model, we can determine the slit half-width, x, and the geometric surface area of the micropore walls, S_g, by,

$$x = k_0/E_0 \text{ nm}$$
$$S_g = (W_0/x) \times 10^3 \text{ m}^2/\text{g}$$

where $k_0 = 13.03 - 1.53 * 10^{-5} E_0^{3.5}$ (Dubinin, 1981).

Typical D-R plots are shown in Fig. 5 for PS-DVB-800 carbons. It can be seen that very good linear relationships are obtained in all cases. Since the intercepts of the D-R plots to the vertical axis for $\log(V)$ reflect the micropore volumes, the obvious influence in activation on pore structure can be observed.

Table 2 lists the micropore and mesopore structural parameters of some selected samples obtained from D-R approach and mercury porosimetry. Macropore (>500 Å) structural parameters are not included because it was found that both non-activated and activated PS-DVB carbons contain essentially no macropores and the fact that the contribution of macropores to the effective pore system is negligible.

The results in Table 2 show that the extent of micropores (W_0) have been greatly developed by activation in CO_2. The micropore development is accompanied by a slight progressive pore widening during activation, i.e., a slight increase in the half-width of the slit-shaped micropores (x). It should be noted though that the half-width initially decreases, due to the presence of newly developed micropores of smaller size. It appears that the size of micropores and the extent of micropore widening, is larger for chars activated at 800°C than for those burned-off at 850°C. This might be an indication that at high burnoff levels, the micropore structure of PS-DVB-800 could collapse more readily than PS-DVB-850, as observed in Fig. 4. The micropore surface areas (S_g), reported in Table 2, increase substantially with activation in the range studied. Another way of examining the micropore structure of these types of carbons is by the use of the Horvath-Kawazoe equation (1983). Figure 6 is one such plot (for PS-DVB-800; 33% BO), it is noted that the Horvath-Kawazoe equation leads to a smaller micropore size distribution than the Dubinin-Radushkevich equation for these materials.

Mesopore structural parameters obtained from mercury porosimetry are also listed in Table 2. From these data, it is obvious that the carbonized PS-DVB already contains a relatively large volume and area in mesopores and the extent of increase in mesopore volume and surface area with burnoff is not so prominent as that for micropores. It should be noted that the surface areas (as high as 192 m^2/g) and pore volume of mesopores (as large as 0.442 cm^3/g) are very high compared to activated carbons derived from natural products (coal,

Table 2. Pore structural parameters of PS-DVB carbons (activated at 800 and 850°C).

Sample	BO (wt%)	Micropores (D-R Eq.)			Mesopores (Hg porosimetry)	
		x (nm)	W_0 (cm^3/g)	S_g (m^2/g)	S_{meso} (m^2/g)	V_{meso} (cm^3/g)
PS-DVB-800	0	0.702	0.077	110	70.3	0.199
	23.9	0.548	0.287	524	97.0	0.252
	33.3	0.610	0.378	620	133	0.343
	42.3	0.682	0.464	680	191	0.442
PS-DVB-850	22.8	0.515	0.322	626	88.0	0.246
	34.1	0.586	0.379	648	123	0.320
	46.8	0.653	0.508	778	192	0.435

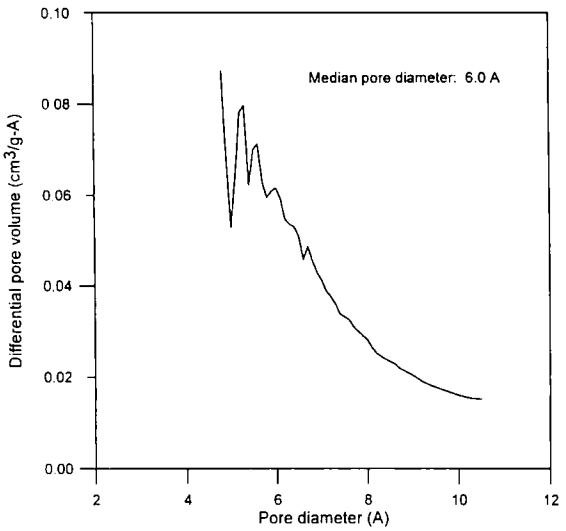

Figure 6. Horvath-Kawazoe differential micropore volume distribution for PS-DVB-800 (BO = 33.3 wt%) carbon.

wood etc.). These unusual features of large mesopore volumes and surface areas of the mesopores in conjunction with extensive micropores make these materials good candidates for applications in which mass transport and surface accessibility play major roles (e.g., catalysis).

When comparing the pore structural parameters of these carbons produced at different activation temperatures, it can be seen that for similar burnoff levels, for micropores, PS-DVB-800 carbons have larger pore sizes, smaller pore volume and surface area than do the PS-DVB-850 carbons. However for mesopores, the pore volume and surface area are larger for PS-DVB-800 than for PS-DVB-850. It should be pointed out that although activation temperature has some effect on the pore structure development, it is not very significant, under the conditions studied. It is the burnoff level that really dominates the pore structure of these porous carbons, as also demonstrated by others (Marsh and Rand, 1971; Dubinin and Stoeckli, 1980).

Figure 7 compares the mesopore size distributions from mercury porosimetry for PS-DVB-800 carbons at various activation stages. As seen in Fig. 7, essentially no pores larger than 200 Å exist in these carbons. The mesopores before activation (BO = 0 wt%) are centered around 90 Å and when activation proceeds, the distribution peak moves slightly toward smaller pore sizes. Presumably, new mesopores of smaller sizes are being generated through widening of the existing and newly developed micropores. Only a very slight

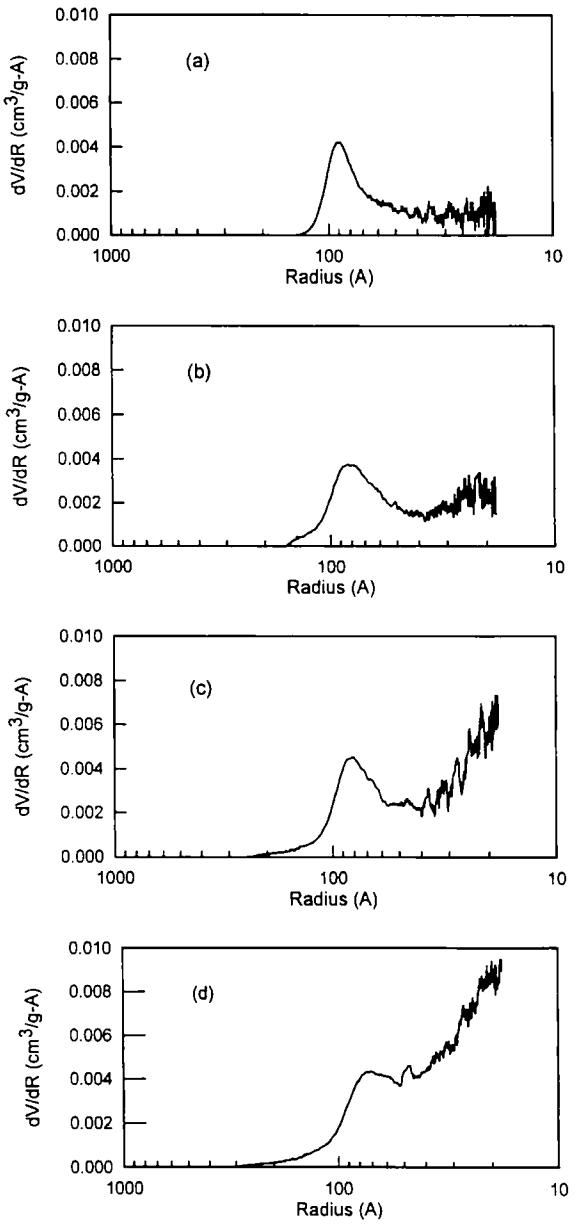

Figure 7. Mesopore size distributions for PS-DVB-800 carbons from mercury porosimetry (a) BO = 0 wt%; (b) BO = 23.9 wt%; (c) BO = 33.3 wt%; (d) BO = 42.3 wt%.

enlargement of the original mesopores (longer tail toward larger pore size) can be observed. Thus, the original mesopore nature of the carbonized PS-DVB char is essentially maintained during activation, which, of course, leads to enhanced microporosity.

Limited data from Scanning Electron Microscopy (SEM) studies indicated that the particles are spherical, and that there is a particle size reduction during

activation at higher burnoff level indicating the occurrence of some removal of the external surface of carbon. Sieving analysis showed that for both PS-DVB-800 and PS-DVB-850 carbons, the particle size almost does not change below 30% BO, with the weight averaged diameter around 364 μm. Further activation leads to a decrease in particle size, for example, the particle size for PS-DVB-800 is 345 μm at 42.3% BO and 327 μm at 65.9% BO. For PS-DVB-850, it is 295 μm at 46.8% BO and 284 μm at 86.8% BO. Density measurements in H_2O show that all the porous carbons made have a skeletal density close to 1.80 g/cm^3. Very little variation with burnoff is observed. Qualitatively, these PS-DVB carbons are mechanically strong, they are difficult to crush manually and probably very resistant to abrasion.

3.4. *Surface Oxygen Functionality Studies*

It is well accepted that the adsorption behavior of carbons can be highly influenced by surface oxygen groups, especially those of acidic nature. Thermal desorption of these oxygen groups, which are fixed firmly on carbon surface, yield CO_2, CO and H_2O. The most dominant oxygen groups which evolve CO_2 (CO_2-complexes) upon decomposition have been identified as carboxyls and lactones, and those which evolve only CO (CO-complexes) are carbonyls, phenols, or quinones. Some groups such as carboxylic anhydrides can desorb both CO_2 and CO, presumably concurrently. The CO_2-complexes are mainly responsible for the acidity of the carbon surface (Otake and Jenkins, 1993). Phenol is the only CO-complex that displays noticeable acidity. The thermal stability of the oxygen groups are characteristic of their chemical structure and/or the heterogeneity of the carbon surface. As examples, studies have shown carboxyls desorb at temperature as low as 125°C, with maximum evolution rate near 300°C (Otake and Jenkins, 1993). The decomposition range for lactones is 150–625°C (Marchon et al., 1988), with evolution peaking at about 325°C (Calo and Hall, 1989). CO-complexes such as carbonyls, phenols, and quinones are quite stable and can only be desorbed at temperatures over 625°C (Bansal et al., 1988; Calo and Hall, 1989). For carboxylic anhydride groups, both evolution peaks at 325°C (Calo and Hall, 1989) and 625–825°C (Otake and Jenkins, 1993) have been reported.

In this investigation, carbon surfaces have been modified systematically by HNO_3 and H_2O_2-oxidation and by subsequent heat treatment at various conditions for an oxidized PS-DVB (PS-DVB-800, BO = 33.3 wt%) carbon and oxidized Ambersorb 575. Effects such as oxidation method, pore structure of carbon, oxidation time and temperature, and subsequent heat treatment, on the surface oxygen functionality development have been studied. Through LTPD, and selective neutralization experiments, the carbon surface nature, particularly the acidic nature, was characterized both quantitatively and qualitatively. A comparison of some of the pore structural parameters between the two porous carbon materials is given in Table 3. The data for Ambersorb 575 are those reported by the manufacturer (Rohm and Haas Company, 1992). It is obvious that the pore structures of both materials are remarkably similar. The only appreciable difference is that the PS-DVB carbon contains more mesoporosity than does the Ambersorb material.

Table 3. Comparison of pore structural parameters.

Sample	V_{micro} (cm^3/g)	V_{meso} (cm^3/g)	V_{macro} (cm^3/g)	V_{total} (cm^3/g)	S_{BET} (m^2/g)
PS-DVB-800 (BO = 33.3 wt%)	0.38	0.34	~0	0.72	816
Ambersorb 575	0.32	0.20	0.20	0.72	800

It should be noted that the heating rate used for the temperature program in the LTPD experiments was only 5°C/min. Under these conditions, the concentration of CO_2 and CO are very low, thus, reducing significantly the possibility of secondary reactions which could alter the results. In addition, the amount of water was found to be very small (generally negligible) for all carbons studied. Its evolution was found in the temperature range between 200–550°C. This water is believed to be that adsorbed and/or hydrogen bonded on the carbon surface. Other sources of H_2O evolution from, for example, condensation of phenolic groups can only desorb at temperature above 625°C. The observation of little or no water evolved at high temperatures suggest that phenolic groups are in very low concentrations or are absent from the samples examined. Therefore, for these samples, the CO_2 and CO evolved reflect the extent and nature of the oxygen groups on the carbon's surface.

3.4.1. Effect of Oxidation Medium and Pore Structure. Figure 8 presents typical LTPD curves for PS-DVB-800 carbon (BO = 33.3 wt%) and Ambersorb 575 oxidized at 60°C for 4 h in HNO_3 or H_2O_2. In

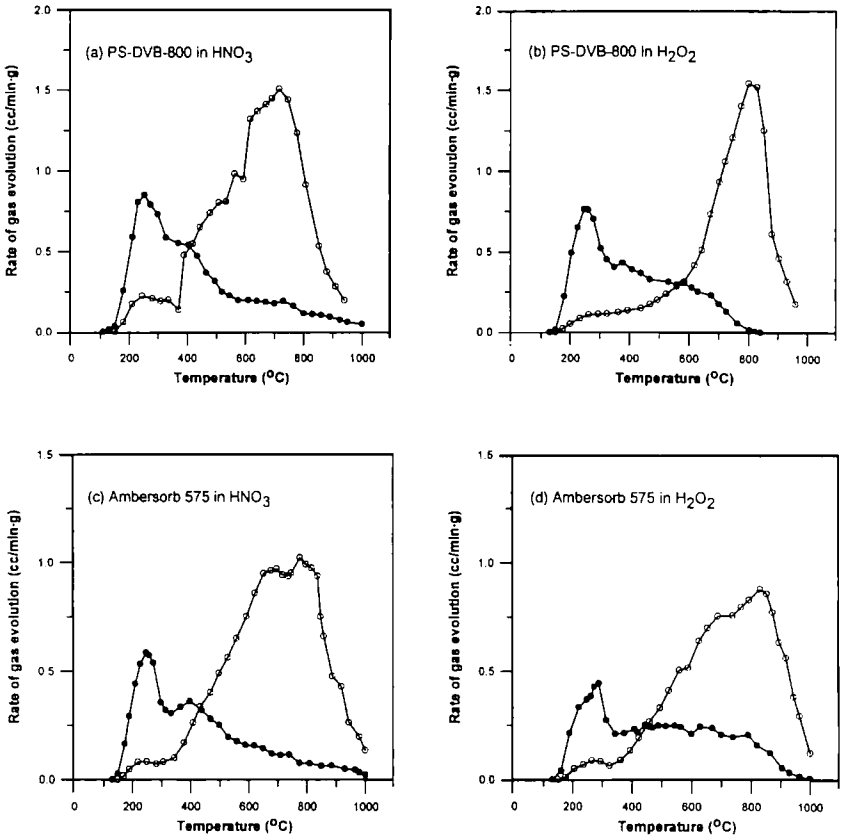

Figure 8. Gas evolution profiles (CO_2, -●-●-, CO, -○-○-) for HNO_3 or H_2O_2-oxidized (60°C, 4 h) PS-DVB-800 (BO = 33.3 wt%) and Ambersorb 575 carbons.

all cases, gas evolution is almost complete at 1000°C. Although certain differences can be discerned, all the gas evolution profiles exhibit essentially very similar patterns, indicating the oxygen groups on these carbons have very similar chemical structures regardless of the oxidation method and the type of carbon used. Each gas evolution profile for CO_2 or CO has two distinct regions. The LTPD curves for CO_2 have large evolution peaks that pass through maxima at about 250°C, and then shoulders and tail region from about 350°C to 1000°C. The evolution profiles for CO have a very small peak near to 250°C, followed by a large, wide evolution peak up to 1000°C, centered around 750°C (although slight difference exists among these samples). The first CO_2 peak at 250°C suggests the existence of carboxyl groups (Otake and Jenkins, 1993) and/or lactone groups (Calo and Hall, 1989), and the shoulder and tail region strongly implies that carboxylic anhydrides are present. The first CO peak is very small and may be relatively unstable carboxylic anhydrides on the carbon surface since other CO-complexes usually evolve at much higher temperatures. Since it is more important to characterize the major oxygen groups present in relatively large amount on the carbon surface, especially those acidic groups, this peak is not of great interest and will not be elaborated on further. The second CO peak, is then at least partially derived from carboxylic anhydrides, which concurrently evolve CO_2, and contributions from carbonyls and quinones.

Differences in the total amounts of CO_2 and CO evolved, and relative amounts of oxygen groups evolved at different temperature ranges among these samples can also be seen in Fig. 8. For each carbon (PS-DVB-800 or Ambersorb 575), more oxygen groups are introduced onto the carbon surface by HNO_3 oxidation than by H_2O_2. This is most obvious for PS-DVB-800 (Figs. 8(a) and (b)) than Ambersorb 575 (Figs. 8(c) and (d)). The LTPD data reveals the total oxygen groups desorbed from HNO_3 and H_2O_2 oxidized PS-DVB-800 is 6.60 mmol/g and 4.95 mmol/g, respectively, and that from HNO_3 and H_2O_2 oxidized Ambersorb 575

Table 4. Effect of oxidation time and temperature on oxygen groups and total acidity for PS-DVB-800 (BO = 33.3 wt%) carbon oxidized at 60°C (and 20°C) for various times.

Time	CO_2 (mmol/g)	CO (mmol/g)	Total-O[a] (mmol/g)	CO_2/Total-O	Acidity[b] (mmol/g)	Acidic/Total-O[c]
H_2O_2, 1 h	1.63 (1.14)	2.90 (2.41)	4.53 (3.55)	0.36 (0.32)	1.15 (0.81)	0.25 (0.23)
H_2O_2, 4 h	1.81	3.14	4.95	0.37	1.53	0.31
H_2O_2, 8 h	1.85 (1.28)	3.31 (2.87)	5.16 (4.15)	0.36 (0.31)	1.77 (0.90)	0.34 (0.22)
H_2O_2, 12 h	1.88	3.60	5.48	0.34	2.01	0.37
H_2O_2, 18 h	2.58	3.74	6.32	0.41	2.37	0.38
H_2O_2, 24 h	2.24	4.10	6.34	0.35	2.90	0.46
HNO_3, 1 h	1.72 (0.99)	3.38 (3.08)	5.10 (4.07)	0.34 (0.24)	2.44 (1.46)	0.48 (0.36)
HNO_3, 4 h	2.16	4.44	6.60	0.33	3.07	0.47
HNO_3, 8 h	2.71 (1.19)	5.31 (3.74)	8.02 (4.93)	0.34 (0.24)	3.69 (1.60)	0.46 (0.33)
HNO_3, 12 h	3.31	5.67	8.86	0.37	4.01	0.45
HNO_3, 18 h	3.08	6.05	9.07	0.34	4.09	0.45
HNO_3, 24 h	3.34	6.05	9.39	0.36	4.44	0.47

[a]Total-O = CO_2 + CO, i.e., total oxygen groups desorbed.
[b]Acidity = total acidity as determined by NaOH.
[c]Acidic/Total-O = Acidity/Total-O, fraction of acidic groups in the total oxygen groups.

is 4.82 mmol/g and 4.34 mmol/g, respectively. For the same oxidation method, more oxygen groups are present on PS-DVB-800 than on Ambersorb 575 for either HNO_3 or H_2O_2 treatment. This probably indicates less structural order in the PS-DVB samples than the Ambersorb. Furthermore, it has been found for PS-DVB-800 carbons prepared at burnoff levels varying from 0 wt% to 42.3 wt% (in CO_2), when subsequently oxidized with HNO_3 or H_2O_2, the oxygen groups increase with burnoff at the same oxidation conditions. As an example, for 4 h oxidation at 60°C in HNO_3, the oxygen groups added to PS-DVB-800 carbons increase from 4.33 mmol/g to 8.28 mmol/g as the burnoff level increases from 0 wt% to 42.3 wt%. This is probably explained by the increased microporosity, and mesoporosity, with higher burnoff for PS-DVB-800 carbons.

The prior trends also apply to the total acidic groups, determined by neutralization with NaOH, on these carbons. This is due to the observation that acidic groups are found to increase monotonically (although in some cases not linearly) with the increase in the total oxygen groups formed by HNO_3 and H_2O_2 oxidation, which can be seen in Table 4.

3.4.2. Effect of Oxidation Time and Temperature on Oxygen Groups. Table 4 lists the results from LTPD and neutralization experiments for PS-DVB-800 (BO = 33.3 wt%) oxidized by HNO_3 and H_2O_2 at 60°C and 20°C for various times. Data in the parentheses are values obtained for oxidations at 20°C. It is very clear that for either oxidation method, increasing the oxidation time will increase both oxygen groups and the total acidity of the carbon. For example, the total amount of oxygen groups and total acidic groups have increased from 5.10 mmol/g and 2.44 mmol/g respectively to 9.39 mmol/g and 4.44 mmol/g for HNO_3 oxidations varying from 1 to 24 h. For H_2O_2 oxidation, the total oxygen groups and the total acidic groups have been increased from 4.53 mmol/g and 1.15 mmol/g respectively to 6.34 mmol/g and 2.90 mmol/g from 1 to 24 h. These data again show the more significant influence of HNO_3 in its ability to oxidize carbon surfaces.

For HNO_3 oxidation, the CO_2/Total-O ratio remains quite constant with oxidation time, with an average value about 0.35. This indicates that the CO_2-complexes increase linearly with amount of total oxygen groups. The ratio of total acidity to total oxygen group concentration (Acidic/Total-O, Table 4) does not vary with oxidation time, with an average value of 0.46. This also indicates that the acidic groups increase linearly with total oxygen groups, and hence, the CO_2-complexes. For H_2O_2 oxidation, the same trends can be found for CO_2/Total-O ratio, which averages 0.37 and is very close to that for HNO_3 oxidation (0.35). However, the Acidic/Total-O ratio increases monotonically with oxidation time from 0.25 to 0.46, showing that

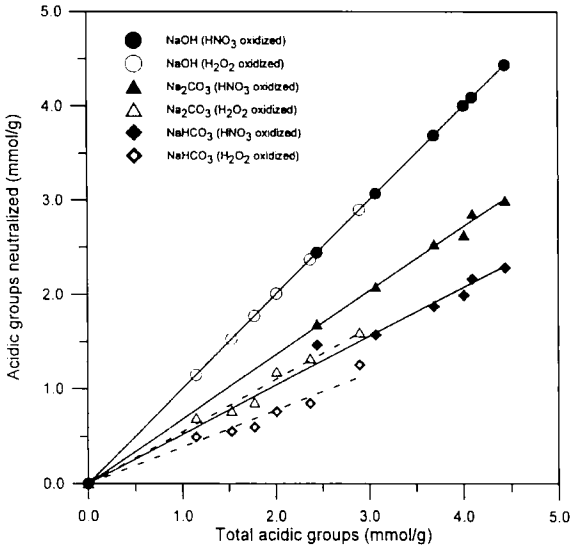

Figure 9. Amounts of acidic groups neutralized by NaOH, Na_2CO_3, and $NaHCO_3$ as a function of total concentration of acidic sites for HNO_3 and H_2O_2 oxidized PS-DVB-800 carbons.

H_2O_2 oxidized carbons contain higher specific acidity at higher surface coverages.

Further information on the nature of the oxygen-groups can be obtained by neutralizing the carbon's surface with different bases. In these studies selective neutralization was made with NaOH, Na_2CO_3 and $NaHCO_3$. It has been proposed (Boehm, 1966) that the predominant neutralization sequence is: only carboxyl groups are neutralized by $NaHCO_3$, lactones and carboxyls by Na_2CO_3, and all acidic groups neutralized by NaOH. Thus, the difference between $NaHCO_3$ and Na_2CO_3 data will be a measure of the lactone-type groups. Likewise, the difference between the Na_2CO_3 and NaOH data will represent the weakest acidic groups present.

The results of these experiments are presented in Fig. 9. In this figure the concentration of acidic groups neutralized by the particular base is plotted versus the concentration of all acidic sites on a given carbon as determined by NaOH neutralization. Thus, the plot of acidic groups neutralized by NaOH for the various oxidized carbons as a function of total acidic groups is a straight line with a slope of unity. It is included to indicate total acid groups on each type of oxidized carbon. From the figure it is obvious that the data for both sets of oxidized carbons fall on reasonably straight lines, although there is a quite strong suggestion that the values lie on an upward curve. Linear regression analysis for all these lines show that for the worst case, $R^2 = 0.991$.

For the HNO_3-oxidized samples it is clear that approximately half (52%) of the acidity can be attributed to carboxyl groups and slightly more than 15% of the acidity is due to lactone-type. On the other hand, for H_2O_2 treated samples the combined carboxyl/lactone groups only constitute just over half (55%) the total acidic groups. Treatment in H_2O_2 only produces about 39% of the acidic groups as carboxyls and 16% lactones. These results indicate that it is possible to modify, and to some extent tailor, the extent and specific nature of the oxygen-containing groups on carbon. These differences will lead to changes in adsorption performance and possible lead to the use of modified carbons as ion-exchange materials.

The influence of temperature on oxidation by HNO_3 and H_2O_2 is as would be anticipated (Table 4). Oxidations carried out at the lower temperature (20°C) for a given time produce lesser quantities of oxygen-containing groups than is found for treatment at 60°C. It appears that the ratios of CO_2/Total-O and Acidity/Total-O are lower at 20°C than produced at 60°C, indicating that CO-evolving groups are favored over the more acidic CO_2-evolving groups at these conditions. This effect appears to be more pronounced for HNO_3 treatment than for H_2O_2 oxidation. Although limited in scope, these results suggest that oxidation temperature, as well as oxidation reagent is an important variable in determining the nature and extent of the oxygen-containing groups that can be produced on a particular carbon's surface.

4. Conclusions

Porous carbons with bimodal pore size distribution have been produced from a commercially available mesoporous styrene/divinylbenzene copolymer. Preoxidation of this polymer in air, prior to pyrolysis, is very important in increasing the carbon yield and maintaining the thermosetting properties of the polymer. In this fashion, the mesoporous nature of the polymer is maintained during the preparation of the carbon. Although activation temperature (in CO_2) has a significant effect on char reactivity, it also influences the pore structure during the activation process. However, as would be anticipated, the most important factor in generating porous carbons of different pore structures is burnoff level. Experimental results from pore structure characterization and surface oxygen functionality studies suggest that the porous carbons produced have an extensive bimodal pore size

distribution and extensive surface area (or active sites) suitable for applications such as adsorption and catalysis. Surface oxygen groups on porous carbons can be easily controlled by oxidation in HNO_3 or H_2O_2 at selected conditions. Oxidation in HNO_3 and H_2O_2 develops substantial concentration of oxygen-containing groups with similar chemical structures but with different relative fractions and thermal stabilities. Linear Temperature Programed Desorption (LTPD) and selective neutralization techniques have proved to be simple and useful characterization tools for these materials.

Nomenclature

A	$[= RT\ln(p_0/p)]$ Parameter of the Dubinin-Radushkevich equation	$Jmol^{-1}$
E_0	Characteristic energy	$Jmol^{-1}$
p	Adsorption pressure	Pa
p_0	Saturation pressure of the adsorbate at temperature T	Pa
R	Ideal gas constant	$= 8.314\ Jmol^{-1}K^{-1}$
R_T	Reactivity	$gmin^{-1}g^{-1}$
S_{BET}	BET surface area	m^2/g
S_g	Geometric surface area of the micropore walls	m^2/g
S_{meso}	Surface area of the mesopores	m^2/g
t	Time	min
T	Temperature	K
V	Volume of adsorbate at standard temperature and pressure	cm^3/g
V_{macro}	Total volume of the macropores	cm^3/g
V_{meso}	Total volume of the mesopores	cm^3/g
V_{micro}	Total volume of the micropores	cm^3/g
V_{total}	Total pore volume	cm^3/g
w	Weight of char	g
W	Micropore volume filled at temperature T	cm^3/g
W_0	Total volume of the micropores, same as V_{micro}	cm^3/g
x	Half width of the micropores	nm

Greek Letters

β	Affinity coefficient of the adsorbate	
$\tau_{0.5}$	Time to reach 50 wt% burnoff	min

References

Bansal, R.C., J.B. Donnet, and F. Stoeckli, *Active Carbon*, Marcel Dekker, New York, 1988.

Boehm, H.P., in *Advances in Catalysis*, E.D. Eley, H. Pines, and P.B. Weisz (Eds.), Vol. 16, p. 179, Academic Press, New York, 1966.

Calo, J.M. and P.J. Hall, *Preprints of Papers Presented at the 197th ACS National Meeting*, Vol. 34, p. 71, American Chemical Society, 1989.

Cronauer, D.C., R.G. Ruberto, R.S. Silver, R.G. Jenkins, I.M.K. Ismail, and D. Schlyer, *Fuel*, **62**, 1116 (1983).

Dubinin, M.M., *Carbon*, **19**, 321 (1981).

Dubinin, M.M., in *Chemistry and Physics of Carbon*, P.L. Walker, Jr. (Ed.), Vol. 2, p. 51, Marcel Dekker, New York, 1966.

Dubinin, M.M., in *Progress in Surface and Membrane Science*, D.A. Cadenhead (Ed.), Vol. 9, p. 1, Academic Press, London, 1975.

Dubinin, M.M. and H.F. Stoeckli, *J. Colloid Interface Sci.*, **75**, 34 (1980).

Gregg, S.J. and K.S.W. Sing, *Adsorption, Surface Area and Porosity*, p. 25, Academic Press, London, 1982.

Hall, P.J., J.M. Calo, H. Teng, E.M. Suuberg, J.A. May, and W.D. Lilly, *Preprints of Papers Presented at the 197th ACS National Meeting*, Vol. 34, p. 112, American Chemical Society, 1989.

Horvath, G. and K.J. Kawazoe, *J. Chem. Eng. Japan*, **6**, 470 (1983).

Jenkins, R.G., S.P. Nandi, and P.L. Walker, Jr., *Fuel*, **52**, 288 (1973).

Kawasumi, S., M. Egashira, and K. Uno, *J. Chem. Soc. Japan*, **3**, 403 (1979).

Laurendau, N.M., *Prog. Energy Combust. Sci.*, **4**, 221 (1978).

Mahajan, O.P. and P.I. Walker, Jr., in *Analytical Methods for Coal and Coal Products*, C. Karr (Ed.), Vol. II, p. 465, Academic Press, London, 1978.

Marchon, B., J. Carrazza, H. Heinemann, and G.A. Somorjai, *Carbon*, **26**, 507 (1988).

Marsh, H. and B. Rand, *Carbon*, **9**, 47 (1971).

Neely, J.W. and E.G. Isacoff, *Carbonaceous Adsorbents for the Treatment of Ground and Surface Waters*, Marcel Dekker, New York, 1982.

Neely, J.W., *Carbon*, **19**, 27 (1981).

Neely, J.W., U.S. Patent 4,040,900, 1975.

Otake, Y. and R.G. Jenkins, *Carbon*, **31**, 109 (1993).

Rohm and Haas Company, Technical notes: *Ambersorb Carbonaceous Adsorbents*, Aug. 1992.

Salinas-Martínez de Lecea, C., M. Almela-Alarcón, and A. Linares-Solano, *Fuel*, **69**, 21 (1990).

Walker, P.L., Jr., F. Rusinko, Jr., and L.G. Austin, *Adv. Catal.*, **11**, 134 (1959).

Wall, L.A., in *The Mechanisms of Pyrolysis, Oxidation and Burning of Organic Materials*, L.A. Wall (Ed.), Nat. Bur. Stand. (U.S.), Vol. 357, p. 47, Spec. Publ., Maryland, 1970.

Winslow, F.H. and W. Matreyek, *J. Poly. Sci.*, **XVII**, 315 (1956).

Winslow, F.H., W.O. Baker, N.R. Pape, and W. Matreyek, *J. Poly. Sci.* **XVI**, 101 (1955).